Two large amplitude slowly pulsating hot subdwarf stars

C. Koen[★]

Department of Statistics, University of the Western Cape, Private Bag X17, Bellville, 7535 Cape, South Africa

ABSTRACT

The discovery observations of two new slowly pulsating subdwarf B stars (V1093 Her stars), BPS CS22890−74 and PB 7032, are presented. Both stars are highly multiperiodic, and have – for V1093 Her stars – large amplitudes. Published descriptions of the (wavelength) spectra of the stars conflict, but new spectra show that both are sdB stars with effective temperatures below 30 000 K. BPS CS22890−74 has a cool companion.

Key words: stars: individual: BPS CS22890−74 – stars: individual: PB 7032 – stars: oscillations – subdwarfs.

1 INTRODUCTION

Neither star discussed in this paper can be described as 'well-studied'; each currently has four references listed in the SIMBAD data base.

BPS CS22860−74 (aliases Balloon 081400001, BPS BS16559−0077) was identified as an ultraviolet-excess star by Bixler, Bowyer & Laget (1991). Follow-up optical spectroscopy (3600–7000 Å, 7 Å resolution; or 3800–7200 Å, 10 Å resolution – the setup for individual stars is not given) was then obtained for candidate subluminous objects, including BPS CS22890−74. The spectrum was found to be composite, showing both features of a cool star (*G* band, Mg I) and a hot object (He I and He II lines). The latter set of lines suggests that the hot component could be an sdO star, or a He-rich sdB star.

By contrast, based on their spectrum (3700–4500 Å, 1.2 Å resolution), Beers et al. (1992) classify the star 'sdB', and give equivalent widths of 0.98 and 0.17 Å for the He I 4387 and 4471 lines, respectively. They do not include BPS CS22860−74 amongst the objects they find to be composite. Furthermore, the authors provide a calibration of temperature on the photometric index

$$Q = (U - B) - 0.72(B - V).$$

Using the photometry $V = 13.95$, $(B - V) = 0.09$ and $(U - B) = -0.69$ obtained by Norris, Ryan & Beers (1999), $Q = -0.75$ and a temperature of $T_{\rm eff} \approx 25\,000$ K follows – far below sdO star temperatures. Of course, this pre-supposes that the colour indices have not been contaminated by a hidden cooler companion. However, for a very cool companion, the $(B - V)$ index is the more likely of the two indices to be too red: reducing it would further decrease the derived temperature.

The two-micron all-sky survey (2MASS) near-infrared magnitudes of BPS CS22860−74 are $J = 13.50(0.027)$, $H = 13.38(0.025)$ and $K_S = 13.31(0.037)$ (Skrutskie et al. 2006), where the numbers

★E-mail: ckoen@uwc.ac.za

in brackets are the quoted error sizes. The optical and infrared magnitudes can be combined to give colour indices which can be compared to those of single and composite hot subdwarfs, as presented by Stark & Wade (2003), and Reed & Stiening (2004). The $(J - K_S)$ and $(V - K_S)$ indices suggest a cool companion (see e.g. fig. 1 in Stark & Wade 2003), as do colours in a $(J - H)$–$(B - J)$ plot, and various infrared colour–colour diagrams (fig. 1 in Reed & Stiening 2004). The star is also well within the area occupied by composite stars in a $(J - H)$–$(V - J)$ plot (Heber 2009, Fig. 6). The relatively red $(B - V)$ index suggests that the spectral type of the companion cannot be very late. (Note that reddening is modest – $E(B - V) < 0.1$ mag – Schuster et al. 2004.)

A low (5 Å) resolution spectrum of BPS CS22890−74, obtained by Robert Czanik (Northwest University, South Africa), is plotted in Fig. 1. The spectrum is the result of a 1200 s exposure with the Grating Spectrograph of the South African Astronomical Observatory (SAAO), which was mounted on the SAAO 1.9 m telescope at Sutherland. The spectrum has been wavelength and flux calibrated.

The general appearance of the spectrum (steep rise at short wavelengths; the width, and depth and number of hydrogen lines) confirms that the star is a hot subdwarf. Interestingly, there are no signs of He absorption. Model fits to the Balmer line profiles, kindly provided by Dr. Stephan Geier (University Erlangen-Nuremberg, Germany), give $T_{\rm eff} = 29400 \pm 2300$ K and $\log g = 5.6 \pm 0.3$.

Closer scrutiny of the spectrum reveals the presence of Ca K and Na D lines, *G*-band absorption and Mg I features just shortwards of 5200 Å. All these point to the presence of a cool companion to the sdB star. The Na line implies a spectral type later than F, while the strength of the K line, and the weakness of the Mg I features, point to a type earlier than mid-K. In fact, the spectrum bears a strong resemblance to that of EC 14026−2647 (Kilkenny et al. 1997), for which O'Donoghue et al. (1997) derived a spectral typing of sdB+G2.

The reader's attention is drawn to the emission near 5575Å: the same feature was seen in a second spectrum of the star, hence it is probably not an artefact. No ready explanation comes to mind.
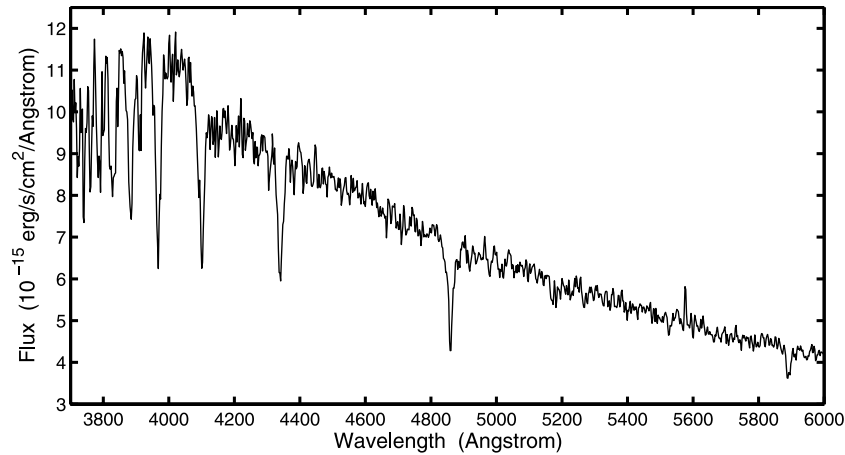
Figure 1. A 5 Å resolution spectrum of BPS CS22890−74.

In addition to the measurements mentioned above there is also published Strömgren (Schuster et al. 2004) and Sloan Digital Sky Survey (Abazajian et al. 2009) photometry of BPS CS22890−74.

The spectrum of PB 7032 (BPS CS22965-31), the second subject of this paper, has also been described as composite. Berger & Fringant (1984) write '... spectrum gives a type sdB; a faint K line and possible emissions at Hβ, Hγ, Hδ suggest a composite or peculiar star...'. As for BPS CS22890−74 above, two-colour diagrams provide a partial check. Strömgren photometry $V = 13.222$, $(b - y) = -0.096$, $m_1 = 0.099$ and $c_1 = -0.041$ was obtained by Kilkenny (1987), and UBV photometry $V = 13.083$, $(B - V) = -0.235$, $(U - B) = -0.666$ by Beers et al. (2007). The latter set of authors estimate the reddening to be low – $E(B - V) = 0.042$ mag. The 2MASS near-infrared magnitudes are $J = 13.61(0.023)$, $H = 13.62(0.034)$ and $K_S = 13.63(0.041)$ (Skrutskie et al. 2006). In this case the star's colour indices lie well within the cloud of single-star values in two-colour diagrams, i.e. there is no photometric evidence that it is composite. Of course, it goes without saying that the near-infrared photometry is only useful for detecting late-type

companions – white dwarfs or other compact objects require other means of detection.

Dr. Elizabeth Green Steward Observatory has generously shared the information that she has obtained six low-dispersion, high signal-to-noise spectra of PB 7032, none of which showed emission features. Professor Gilles Fontaine (Université de Montréal) obtained good non-LTE model fits to the combined spectra with parameters $T_{\rm eff} = 27720 \pm 170$ K and $\log g = 5.5 \pm 0.03$.

PB 7032 has been monitored for rapid variability (15 s time resolution – Østensen et al. 2010a) with negative results.

There are, in fact, two major classes of oscillating sdB stars – rapid pulsators with periods of a few minutes (the EC 14026 or V361 Hya stars; Kilkenny et al. 1997), and slow pulsators with typical dominant periods of 1–2 h (the PG 1716 or V1093 Her stars; Green et al. 2003). A brief summary, in the context of the Extended Horizontal Branch star evolution, can be found in Østensen (2009). The V361 Hya stars are hotter ($T_{\rm eff} > 30\,000$ K), and have higher gravities ($\log g > 5.6$) than the longer period pulsators, but there is some overlap with a few of the hotter V1093 Her stars also showing rapid pulsations (the 'hybrid' or 'DW Lyn' stars). Asteroseismology
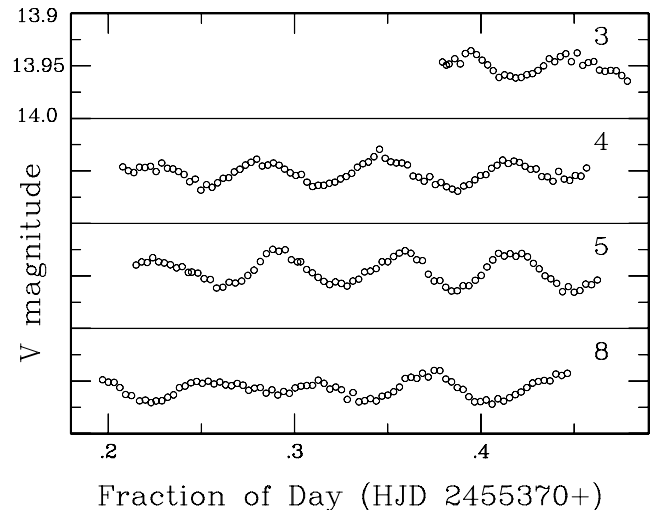
Table 1. The observing logs. Most of the observations were obtained under good photometric conditions, but the seeing was very variable. Given the sparseness of the field, poor seeing was a minor irritant. The minimum number of useful measurements in any filter obtained during each run is given in the last column.

Starting time (HJD 245 5000+)	$T_{\rm exp}$ (s)		Run length (h)	N
	V	R		
BPS CS22860−74				
373.3794	120	90	2.4	33
374.2078	120	90	6.0	82
375.2150	120	90–120	6.0	77
378.1970	120	100	6.0	80
PB 7032				
Starting time (HJD 245 5300+)	$T_{\rm exp}$ (s)		Run length (h)	N
	B	R		
373.5153	120	60	4.2	61
375.4761	120–150	60	5.1	70
463.2725	150	60	2.8	37
467.2347	120–150	60	6.7	95
468.2322	100–150	50-60	7.1	105

Figure 2. *V*-filter light curves of BPS CS22890−74. The vertical width of each panel is 0.1 mag. Panels are labelled with the last digit of the Julian Day of observation.

of these stars is of some interest, as it may be of help to learn about the internal structure of the stars, and thus about their evolutionary history.

The two stars discussed above are new examples of slowly pulsating sdB stars, in terms of both their long periods and their lower effective temperatures.

2 THE OBSERVATIONS

All measurements were made with the SAAO STE4 CCD camera mounted on the SAAO 1.9-m telescope at Sutherland, South Africa. The field of view of the camera on the telescope is 2.4×2.4 arcmin^2. Both starfields are quite sparse, with a single bright comparison star in each case. Measurements of at least one fainter star in the field were also obtained, as a safeguard (e.g. to rule out the possibility that variability originated in the bright comparison stars).
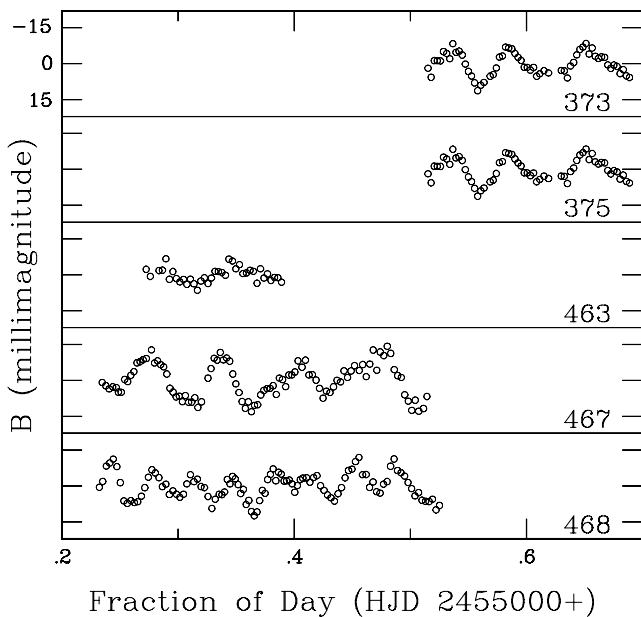

Figure 3. *B*-filter light curves of PB 7032. The vertical width of each panel is 0.044 mag. Individual light curves have been detrended by the subtraction of parabolic fits, in order to lessen the effects of differential extinction. Panels are labelled with the last three digits of the Julian Day of observation.
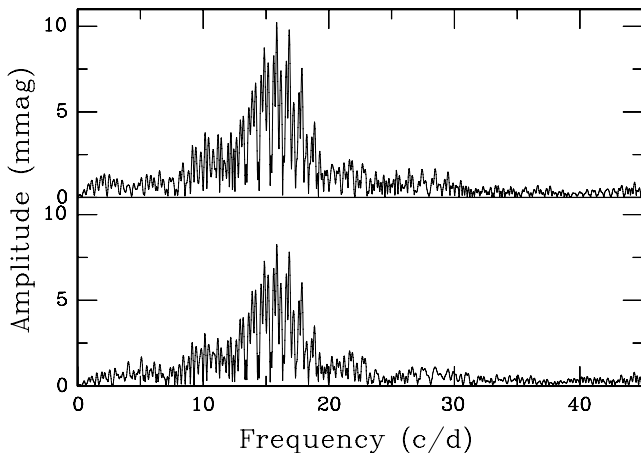

Figure 4. Amplitude spectra of all the BPS CS22860−74 *V*-filter (top) and *R*-filter (bottom) data.

Pre-binning of the images was performed throughout, giving a reasonable readout time of about 17 s.

Observations were cycled through either the *V* and R_C filters (BPS CS22890−74) or the *B* and R_C filters (PB 7032). The R_C filter was selected as it gave good signal-to-noise ratio results for both programme and comparison stars. The comparison star for PB 7032 was bright enough that observations were also obtained through the *B* filter, for which sdB star pulsation amplitudes are expected to be larger than in the red. The BPS CS2280−74 comparison star was fainter, and therefore the *V* filter was used instead. Observations through two filters give two data sets, which, although not entirely independent, at least provide some check on the reality of low-amplitude pulsation frequencies. Restricting observations to two filters still allows good time resolution. The observing logs for the two stars are given in Table 1.

Photometric reductions were performed using an automated version of DOPHOT (Schechter, Mateo & Saha 1993). Both point spread function and aperture magnitudes were obtained: the former were preferred due to the smaller noise levels. Differential measurements with respect to the bright comparison stars were calculated in order to deal with changing atmospheric conditions.

Illustrative light curves of the two stars are plotted in Figs 2 and 3.

3 FREQUENCY ANALYSIS

3.1 BPS CS22890−74

The amplitude spectra of the full BPS CS22860−74 *V*- and *R*-filter data sets are shown in Fig. 4. The results conform to expectations for slowly pulsating sdB in several ways – the frequencies of maximal power, evident multiperiodicity and larger amplitudes at the shorter wavelength.
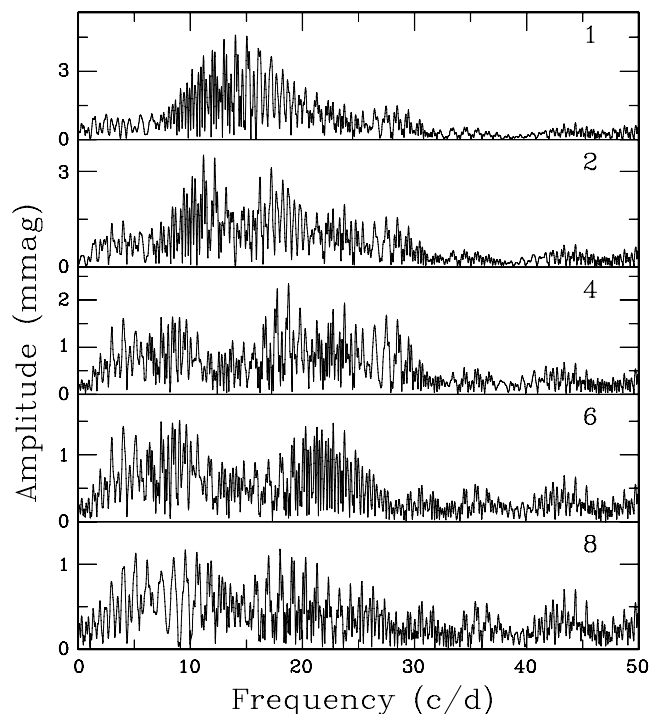

Figure 5. Successive stages of pre-whitening of the BPS CS22890−74 *V*-filter observations. Panels are labelled with the number of sinusoids which have been subtracted from the original data set. Note the different vertical scales of the different panels.

In order to study the frequency content of the data the standard procedure is followed of successive pre-whitening of sinusoids. This consists of (i) finding the frequency at which the periodogram or amplitude spectrum of the data is maximum; (ii) fitting, by ordinary least-squares regression, a sinusoid with this frequency to the data and (iii) subtracting the fitted sinusoid from the observations. Steps (i)–(iii) are repeatedly executed, until it is deemed that all the 'signal' has been extracted from the data.

Two points are worth highlighting. The first is that it is obviously desirable to use an objective measure which can be used to establish at which point to terminate the pre-whitening procedure. Unfortunately, there is currently no statistically rigorous stopping criterion. The method followed here is to compare the results for the two filters, and to retain those frequencies which seem to be common to the two data sets. The second point to be made concerns the word 'seem' in the previous sentence. Random noise gives rise to uncertainties in the frequencies (and, of course, amplitudes and phases) of the sinusoids extracted from the data. A second substantial effect is 'aliasing', or cycle count ambiguities, in the frequencies, induced by the large gaps between the four strings of time series measurements.

The pre-whitening procedure is illustrated in Fig. 5. The top panel shows the amplitude spectrum after pre-whitening by the most prominent frequency identified from the top panel of Fig. 4. Further panels in Fig. 5 give the results of removing further sinusoids. The

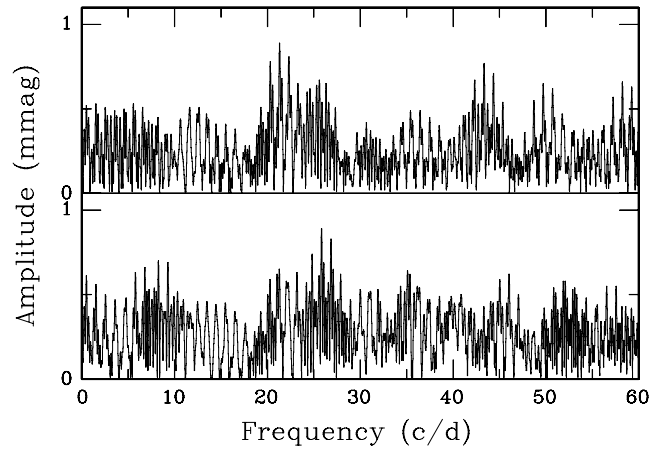**Figure 6.** Amplitude spectra of the residuals after removing nine sinusoids from the *V*-filter (top) and *R*-filter (bottom) BPS CS22860−74 data.

Table 2. The results of successive pre-whitening steps for both BPS CS22860−74 data sets. Frequencies are listed in the order in which they were extracted from the *V*-filter data. The corresponding rank of the frequency in the *R*-filter data is in the fourth column. Formal standard errors of estimates are given in brackets.

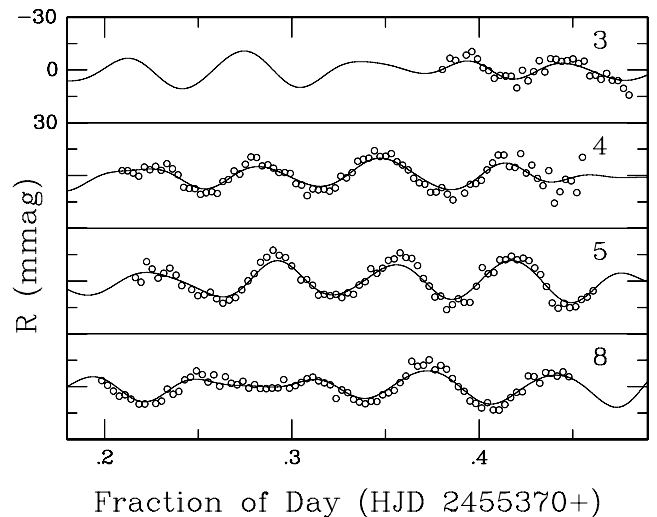|	*V* filter			*R* filter	
	Frequency (d^{-1})	Amplitude (mmag)		Frequency (d^{-1})	Amplitude (mmag)
1	15.872 (0.005)	10.4 (0.5)	1	15.878 (0.006)	8.2 (0.4)
2	14.03 (0.010)	4.7 (0.4)	2	13.00 (0.012)	3.5 (0.4)
3	11.18 (0.011)	3.6 (0.4)	3	11.15 (0.014)	2.7 (0.3)
4	17.26 (0.015)	2.4 (0.3)	5	17.21 (0.013)	2.3 (0.3)
5	18.77 (0.014)	2.3 (0.3)	4	17.73 (0.014)	2.4 (0.3)
6	27.48 (0.018)	1.7 (0.3)	9	28.43 (0.022)	1.2 (0.2)
7	9.05 (0.019)	1.5 (0.3)			
8	22.76 (0.019)	1.4 (0.3)	10	21.73 (0.031)	0.8 (0.2)
9	18.02 (0.022)	1.2 (0.2)			
10	10.58 (0.020)	1.2 (0.2)			

Figure 7. *R*-filter light curves of BPS CS22890−74, with the fit described by the nine sinusoids summarized in Table 3. The vertical width of each panel is 0.06 mag. Panels are labelled with the last digit of the Julian Day of observation.

Table 3. The results of the simultaneous fitting of nine sinusoids to each of the two BPS CS22860−74 data sets. Formal errors of estimated parameters are given in brackets.

	V filter			*R* filter	
Frequency (d^{-1})	Amplitude (mmag)	Phase (rad)	Frequency (d^{-1})	Amplitude (mmag)	Phase (rad)
15.855 (0.005)	9.5 (0.3)	1.37 (0.05)	15.863 (0.007)	7.5 (0.4)	1.32 (0.08)
13.996 (0.006)	5.5 (0.3)	−1.36 (0.10)	13.995 (0.010)	4.2 (0.3)	−1.28 (0.16)
11.197 (0.009)	2.7 (0.2)	−1.66 (0.14)	11.178 (0.013)	2.1 (0.3)	−1.38 (0.21)
17.232 (0.014)	2.9 (0.3)	2.72 (0.16)	17.218 (0.028)	2.3 (0.3)	2.96 (0.27)
18.746 (0.010)	2.5 (0.2)	2.16 (0.15)	18.751 (0.017)	1.9 (0.3)	2.14 (0.23)
27.465 (0.011)	1.7 (0.2)	0.16 (0.21)	27.440 (0.019)	1.1 (0.2)	0.43 (0.36)
22.764 (0.012)	1.7 (0.2)	−0.03 (0.22)	22.751 (0.016)	1.5 (0.2)	0.02 (0.29)
8.386 (0.014)	1.6 (0.2)	−2.90 (0.24)	8.406 (0.018)	1.4 (0.2)	−3.48 (0.31)
4.006 (0.020)	1.0 (0.2)	−2.02 (0.36)	4.036 (0.016)	1.4 (0.3)	−2.67 (0.28)

procedure was terminated after the extraction of 10 frequencies, since no further apparent correspondences between frequencies in the data for the two filters were seen. Note that there is substantial residual power left below $30\,\mathrm{d}^{-1}$ in the spectrum at the bottom of Fig. 5: compare the level of the spectrum at higher frequencies, averaging below 0.5 mmag.

The results for the two filters are summarized in Table 2. Frequencies are listed in the order in which they have been extracted from the V data, with the corresponding ranking in the R data given in Column 4. There is no feature in the R data corresponding to frequency 7 ($9.05\,\mathrm{d}^{-1}$) in the V data. In a number of cases (V-filter frequencies 2, 5, 6 and 8) $1\,\mathrm{d}^{-1}$ aliases are seen in the R-filter data.

The next step in the analysis was to use the set of seven common frequencies as starting values for a non-linear least squares (NLS) procedure which iteratively re-determined best-fitting frequencies, amplitudes and phases for all values simultaneously. Note that the same aliases were used as input for both data sets, V and R. The residuals left after convergence of the NLS algorithm were again subjected to a sequential linear least-squares pre-whitening procedure, which led to the identification of a further two common frequencies – 8.39 and $3.99\,\mathrm{d}^{-1}$ in V and 8.41 and $4.03\,\mathrm{d}^{-1}$ in R.
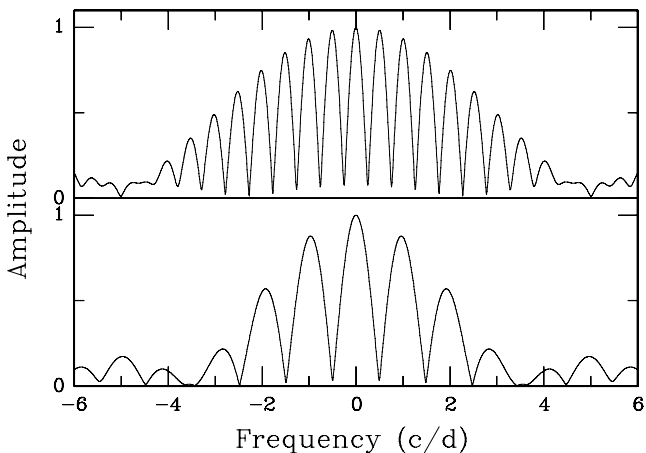

Figure 8. The window functions of the first two nights (top panel) and last two nights (bottom panel) of observations of PB 7021.
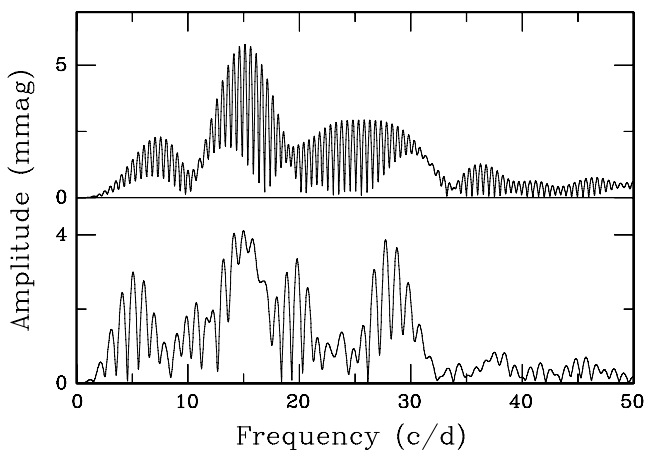

Figure 9. Amplitude spectra of the combined first two nights (top panel) and last two nights (bottom panel) of PB 7032 observations through the B filter. Individual runs were first pre-whitened by subtracting parabolic fits. Note the different vertical scales on the two panels.

Finally, all nine frequencies, with associated amplitudes and phases, were simultaneously fitted to the data by the NLS method, with the results given in Table 3. Note that the lowest frequency ($\sim 4\,\mathrm{d}^{-1}$) is almost certainly an artefact, induced by differential extinction (since BPS CS22890−74 is much bluer than the comparison star). This frequency aside, V-filter amplitudes are consistently a little larger than those seen in R, as expected. Note also that, within the errors, variations measured through the two filters are in phase.

The amplitude spectra of the residuals of the NLS procedure are plotted in Fig. 6: clearly all prominent features common to the two data sets have been removed. The reader's attention is also drawn to the fact that with the exception of the $4\,\mathrm{d}^{-1}$ variation in V, all terms in Table 3 have amplitudes at least a factor of 3 larger than the mean noise level. The R-filter fit is illustrated in Fig. 7.

3.2 PB 7032

A glance at Fig. 3 shows that the time spacing of the PB 7032 data is awkward – two sets of runs, separated by about 3 months. There are also gaps within the two sets of runs. A sensible approach seems to be to separately combine the first two nights, and last two nights of observation – this gives two independent data sets, for which the aliasing is not too complicated (see Fig. 8). Amplitude spectra of the B-filter observations for the two two-night data sets are plotted in Fig. 9. The spectrum in the bottom panel, in particular, suggests the presence of at least four modes with frequencies higher than $10\,\mathrm{d}^{-1}$.

Table 4. The results of the successive frequency pre-whitening of the PB 7032 data. Frequencies are given in d^{-1}, followed by the amplitude in millimagnitudes (in brackets).

| Frequencies in the order of extraction | | | |
| First two nights | | Last two nights | |
B	*R*	*B*	*R*
15.13 (5.8)	15.64 (5.0)	14.99 (4.1)	27.74 (3.5)
27.81 (3.4)	27.83 (3.6)	27.75 (3.8)	15.88 (3.2)
21.89 (2.1)	11.87 (2.3)	15.49 (3.5)	15.40 (2.9)
11.95 (1.6)	21.42 (1.8)	19.86 (2.9)	19.87 (2.2)
5.05 (1.5)	31.05 (1.2)	5.06 (2.7)	11.29 (1.4)
30.07 (1.4)	4.49 (1.1)	11.76 (1.4)	22.15 (1.0)
5.81 (0.8)	38.32 (0.9)	30.86 (1.4)	29.21 (1.0)
16.69 (0.7)	24.27 (0.7)	29.35 (1.4)	4.59 (0.8)
0.25 (2.1)	46.69 (0.7)	23.05 (1.0)	25.79 (0.8)
32.85 (0.6)	8.25 (0.5)	13.17 (0.8)	30.82 (0.6)
47.82 (0.5)	33.42 (0.5)	2.04 (0.7)	14.00 (0.6)
22.80 (0.5)	13.67 (0.4)	21.49 (0.7)	19.48 (0.5)
37.29 (0.4)	43.33 (0.4)	26.90 (0.6)	33.24 (0.5)
Selected frequencies, in the order of *B*-filter extraction			
First two nights		Last two nights	
B	*R*	*B*	*R*
15.1 (5.8)	15.6 (5.0)	15.0 (4.1)	15.9 (3.2)
27.8 (3.4)	27.8 (3.6)	27.8 (3.8)	27.7 (3.5)
21.9 (2.1)	21.4 (1.8)	15.5 (3.5)	15.4 (2.9)
12.0 (1.6)	11.9 (2.3)	19.9 (2.9)	19.9 (2.2)
30.1 (1.4)	31.1 (1.2)	11.8 (1.4)	11.3 (1.4)
16.7 (0.7)	13.7 (0.4)	30.9 (1.4)	30.8 (0.6)
32.9 (0.6)	33.4 (0.5)	29.4 (1.4)	29.2 (0.8)
22.8 (0.5)	24.3 (0.7)	23.1 (1.0)	22.2 (1.0)
37.3 (0.6)	38.3 (0.5)	13.2 (0.8)	14.0 (0.6)
		21.5 (0.7)	19.5 (0.5)
		26.9 (0.6)	25.8 (0.5)

It is clear that the data do not lend itself to the extraction of definitive frequencies. None the less, for the sake of completeness, the results of successive frequency pre-whitening are given in Table 4, for the two two-night data combinations. Results are given for each of the two filters. In the first part of the table the frequencies are given in the order in which they were extracted.

In the second part of Table 4, frequencies below $10\,\mathrm{d}^{-1}$ and above $40\,\mathrm{d}^{-1}$ are excluded. [Low frequencies may be the result of residual differential extinction, while 'real' high frequencies would presumably have been found in the search by Østensen et al. (2010a) for rapid pulsations.] Furthermore, the orders of the R-filter frequencies have been adjusted in an effort to match these to the B-filter values,

Table 5. A summary of some of the observables of published PG 1716 stars. All frequencies are quoted if three or fewer have been found, otherwise the range of values is given. Hybrid fast/slowly pulsators (DW Lyn stars) are marked with asterisks; for these only the lower PG 1716-like frequencies are considered. The V magnitudes were taken from Østensen (2006): for HS 0702+6043 and HS 2201+2610 only B magnitudes are available, hence V was estimated assuming $(B - V) \approx -0.35$. The V magnitude of J08656.7+1527 is from Baran et al. (2011a).

Star	V	No. frequencies	Range (d^{-1})	Max. ampl. (mmag)	Ref.
PG 1716+426	14.0	6	15.8–29.4	1.5 (R)	1
*Balloon 090100001	12.1	4	20.7–31.6 (phot)	2.6 (B)	2
		6	14.6–40.1 (spect)		2
PG 0101+039	12.1	3	11.9, 16.5, 32.6	0.5 (MOST)	3
PG 1627+017	12.9	23	9.7–18.9	4.8 (R)	4
PG 1338+481	13.6	13	9.1–40.7	1.9 (R)	5
*HS 0702+6043	~13.7	3	17.8, 23.5, 27.5	3.7 ($F555W$)	6
EC 21324−1346	13.2	9	11.1–28.8	3.1 (B)	7
KPD 0629−0016	14.9	5	12.3–31.4	3.0 (B)	8
*HS 2201+2610	~14.0	1	26.5	1.5 (B)	9
JL 82	12.4	>10(?)	5(?)–25(?)	4.5 (B)	10
LB 1516	13.0	4	12.2–25.7	2.6 (B)	11
PG 0907+123	13.9	7	11.6–24.9	3.8 (B)	12
JL 194	12.4	5	11.0–20.2	4.2 (B)	12
*J080656.7+1527	14.2	2	25.3, 30.9	1.5 ($BG40$)	13
BPS CS22860−74	14.0	8	8.4–27.5	9.5 (V)	
PB 7032	13.2	>4	12(?)–27.8(?)	5.8 (B)	

References: 1 – Reed et al. (2004); 2 – Baran, Pigulski & O'Toole (2008); 3 – Randall et al. (2005); 4 – Randall et al. (2006a); 5 – Randall et al. (2006b); 6 – Lutz et al. (2008); 7 – Kilkenny et al. (2007); 8 – Koen & Green (2007); 9 – Lutz et al. (2009); 10 – Koen (2009); 11 – Koen et al. (2010); 12 – Koen & Green (2010) and 13 – Baran et al. (2011a).

Table 6. A summary of some of the physical properties of published PG 1716 stars. The DW Lyn stars are marked with asterisks. Note that an 'N' under multiplicity only means that no overt sign of a companion star has been detected.

Star	T_{eff} (K)	$\log g$	Refs.	Multiplicity	Period (d)	Refs.
PG 1716+426	26 100–27 500	5.3–5.5	1–3	Y	1.78	2
*Balloon 090100001	28 700–29 450	5.33–5.39	4,5	N		
PG 0101+039	28 300	5.52	6	Y	0.56	7
PG 1627+017	22 900	5.25	8	Y	0.83	2
PG 1338+481	28 200	5.4	9	N		
*HS 0702+6043	28 400	5.35	10	N		
EC 21324−1346	–	–		N		
KPD 0629−0016	26 500	5.5	11	N		
*HS 2201+2610	29 300	5.4	12	N		
JL 82	25 000	5.0	13	Y	0.74	14
LB 1516	26 100	5.4	13	Y	7–27	14
PG 0907+123	26 200–28 100	5.0–5.5	15–18	Y	6.12	2
JL 194	25 200	5.2	19	N		
*J080656.7+1527	28 500	5.4	20	N		
BPS CS22890−74	29 000	5.6	21	Y	Unknown	22
PB 7032	27 700	5.5	23	N		

References: 1 – Saffer et al. (1994); 2 – Morales-Rueda et al. (2003); 3 – Reed et al. (2004); 4 – Oreiro et al. (2004); 5 – Telting et al. (2006); 6 – Randall et al. (2005); 7 – Moran et al. (1999); 8 – Randall et al. (2006a); 9 – Randall et al. (2006b); 10 – Dreizler et al. (2002); 11 – Van Grootel et al. (2010); 12 – Østensen et al. (2001); 13 – Edelmann (2003); 14 – Edelmann et al. (2005); 15 – Moehler, de Boer & Heber (1990); 16 – Billères et al. (2002); 17 – Maxted et al. (2001); 18 – Koen & Green (2010); 19 – Heber et al. (1984); 20 – Baran et al. (2011a); 21 – S. Geier (private communication); 22 – Koen (this paper) and 23 – G. Fontaine (private communication).

bearing in mind aliasing. The author will err on the side of caution, and refrain from drawing any conclusions from the table.

4 CLOSING REMARKS

Although the incidence of V1093 Her-type pulsation in sdB stars may be high, the amplitudes are generally very low (e.g. Østensen et al. 2010c). The pulsation amplitudes of the two new variables are the highest seen in slowly pulsating sdB stars – see Table 5, which is an updated version of table 5 in Koen & Green (2010). The frequency content of the observations of PB 7032 and BPS CS22890−74 is unremarkable, aside from the lowest frequency in the latter star being a little lower than previously seen. (It should be noted though that even lower frequencies have been found in Kepler observations of V1093 Her stars – see e.g. Baran et al. 2011b.) Table 6 contains further information – effective temperatures, gravities and binary periods, where known. The two new discoveries are not unusual in any of these attributes.

The Kepler mission has discovered a further 12 pulsators of this type (Reed et al. 2010; Kawaler et al. 2010; Baran et al. 2011b) and one new hybrid pulsator (Østensen et al. 2010b). The detection level of Kepler is far superior to that currently attainable from the ground, so that typically many more modes are seen in its data. Only two of the amplitudes detected by Kepler exceed two millimagnitudes.

The temperature and gravity determinations of BPS CS22890−74 in Table 6 suggest that the star may have physical properties typical of the hybrid oscillators which show both rapid and slow pulsations. It would therefore be worthwhile to test it for the presence of short period variations.

REFERENCES

Abazajian K. N. et al., 2009, ApJS, 182, 543
Baran A., Pigulski A., O'Toole S., 2008, MNRAS, 385, 255
Baran A., Gilker J. T., Reed M. D., Østensen R. H., Telting J. H., Smolders K., Hicks L., Oreiro R., 2011a, MNRAS, in press
Baran A. et al., 2011b, preprint (arXiv:1103.1666)
Beers T. C., Preston G. W., Shectman S. A., Doinidis S. P., Griffin K. E., 1992, AJ, 103, 267
Beers T. C. et al., 2007, ApJS, 168, 128
Berger J., Fringant A.-M., 1984, A&AS, 58, 565
Billères M., Fontaine G., Brassard P., Liebert J., 2002, ApJ, 578, 515
Bixler J. V., Bowyer S., Laget M., 1991, A&A, 250, 370
Dreizler S., Schuh S., Deetjen J. L., Edelmann H., Heber U., 2002, A&A, 386, 249
Edelmann H., 2003, PhD thesis, Univ. Erlangen-Nürnberg
Edelmann H., Heber U., Altmann M., Karl C., Lisket T., 2005, A&A, 442, 1023
Green E. M. et al., 2003, Ap&SS, 284, 65
Heber U., 2009, ARA&A, 47, 211
Heber U., Hunger K., Jonas G., Kudritzki R. P., 1984, A&A, 130, 119
Kawaler S. D. et al., 2010, MNRAS, 409, 1509
Kilkenny D., 1987, MNRAS, 228, 713
Kilkenny D., Koen C., O'Donoghue D., Stobie R. S., 1997, MNRAS, 285, 640
Kilkenny D., Copley C., Zietsman E., Worters H., 2007, MNRAS, 375, 1325
Koen C., 2009, MNRAS, 395, 979
Koen C., Green E. M., 2007, MNRAS, 377, 1605
Koen C., Green E. M., 2010, MNRAS, 406, 2701
Koen C., Kilkenny D., Pretorius M. L., Frew D. J., 2010, MNRAS, 401, 1850
Lutz R. et al., 2008, in Heber U., Jeffery C. S., Napiwotzki R., eds, ASP Conf. Ser. Vol. 392, Hot Subdwarfs and Related Objects. Astron. Soc. Pac., San Francisco, p. 339
Lutz R., Schuh S., Silvotti R., Bernabei S., Dreizler S., Stahn T., Hügelmeyer S. D., 2009, A&A, 496, 469
Maxted P. F. L., Heber U., Marsh T. R., North R. C., 2001, MNRAS, 326, 1391
Moehler S., de Boer K. S., Heber U., 1990, A&A, 239, 265
Morales-Rueda L., Maxted P. F. L., Marsh T. R., North R. C., Heber U., 2003, MNRAS, 338, 752
Moran C., Maxted P., Marsh T. R., Saffer R. A., Livio M., 1999, MNRAS, 304, 535
Norris J. E., Ryan S. G., Beers T. C., 1999, ApJS, 123, 639
O'Donoghue D., Lynas-Gray A. E., Kilkenny D., Stobie R. S., Koen C., 1997, MNRAS, 285, 657
Oreiro R., Ulla A., Pérez Hernández F., Østensen R., Rodriguez López C., MacDonald J., 2004, A&A, 418, 243
Randall S. K. et al., 2005, ApJ, 633, 460
Randall S. K. et al., 2006a, ApJ, 643, 1198
Randall S. K. et al., 2006b, ApJ, 645, 1464
Reed M. D., Stiening R., 2004, PASP, 116, 506
Reed M. D. et al., 2004, ApJ, 607, 445
Reed M. D. et al., 2010, MNRAS, 409, 1496
Saffer R., Bergeron P., Koester D., Liebert J., 1994, ApJ, 432, 351
Schechter P. L., Mateo M., Saha A., 1993, PASP, 105, 1342
Schuster W. J., Beers T. C., Michel R., Nissen P. E., Garcia G., 2004, A&A, 422, 527
Skrutskie M. F. et al., 2006, AJ, 131, 1163
Stark M. A., Wade R. A., 2003, AJ, 126, 1455
Telting J., Østensen R., Heber U., Augusteijn T., 2006, Baltic Astron., 15, 235
Van Grootel V., Charpinet S., Fontaine G., Green E. M., Brassard P., 2010, A&A, 524, 63
Østensen R. H., 2006, Baltic Astron., 15, 85
Østensen R. H., 2009, Comm. Asteroseismol., 159, 75
Østensen R. H., Solheim J.-E., Heber U., Silvotti R., Dreizler S., Edelmann H., 2001, A&A, 368, 175
Østensen R. H. et al., 2010a, A&A, 513, 6
Østensen R. H. et al., 2010b, MNRAS, 408, L51
Østensen R. H. et al., 2010c, MNRAS, 409, 1470

This paper has been typeset from a TEX/LATEX file prepared by the author.